

## REVIEW

# Three-dimensional Cardiac MR Imaging: Related Techniques and Clinical Applications

Yasuo Amano<sup>1,2\*</sup>, Fumi Yanagisawa<sup>1,2</sup>, Masaki Tachi<sup>2</sup>, Kuniya Asai<sup>3</sup>,  
Yasuyuki Suzuki<sup>4</sup>, Hidenobu Hashimoto<sup>1,5</sup>, Kiyohisa Ishihara<sup>6</sup>, and Shinichiro Kumita<sup>2</sup>

Three-dimensional (3D) cardiac magnetic resonance (MR) imaging has several advantages, including the easy coverage of the entire heart without misregistration, reduction of breath-holding times, and availability for postprocessing reconstruction. These advantages are associated with some techniques such as breath-hold or navigator gating and parallel imaging. However, the image quality of 3D cardiac MR images is compromised by the use of a shorter repetition time and parallel imaging. Thus, a steady-state free precession sequence, contrast agent administration, and presaturation pulses are used to maintain the image quality. In this review, we introduce the MR imaging techniques used in 3D cardiac MR imaging and demonstrate the typical 3D cardiac MR images, followed by discussion about their advantages and disadvantages.

**Keywords:** *three-dimensional imaging, cardiac magnetic resonance imaging, steady-state free precession, gadolinium, fast data acquisition*

## Introduction

Three-dimensional (3D) imaging data acquisition is used in many fields of magnetic resonance (MR) imaging because of its high signal-to-noise ratio (SNR), easy positioning, higher spatial resolution, the reduction of breath-holding times, and availability for multiplanar reconstruction.<sup>1,2</sup> The homogeneous contrast timing between imaging slices is also an advantage of 3D MR imaging.<sup>2</sup> However, the high SNR can be compromised by the use of shorter repetition time (TR), partial (or fractional) echo, higher bandwidth, or parallel imaging. We recommend preserving the advantages of 3D cardiac MR imaging by using steady-state free precession (SSFP), contrast agents, or presaturation techniques.<sup>3–6</sup> Electrocardiogram (ECG) gating or breath-holding technique is used to suppress motion or blurring artifacts. In this review, we describe MR imaging techniques anticipated for 3D cardiac MR imaging and demonstrate clinical examples acquired with 3D cardiac

MR sequences. We aim to describe the advantages and disadvantages of 3D cardiac MR imaging.

## Imaging Techniques Used in 3D Cardiac MR Imaging

### *ECG gating*

ECG gating is always used for cardiac MR imaging irrespective of two-dimensional (2D) or 3D data acquisition. Cine MR imaging is acquired to divide the cardiac cycle into 16–30 phases, and late gadolinium enhancement (LGE) imaging is performed at the “cardiac static” diastolic phase.<sup>3,7</sup> The data acquisition time should be shorter than 100–150 ms to reduce the cardiac motion artifacts even in the diastolic phase.

### *Breath-holding or navigator gating technique*

The breath-holding technique is used to suppress respiratory artifacts in 3D cardiac cine or LGE MR imaging.<sup>8–11</sup> By using 3D data acquisition, the breath-holding time reduces from 10–14 to 1 or 3 on cine imaging, leading to a shorter examination time. By contrast, other 3D cardiac MR imaging requiring high spatial resolution, such as coronary MR angiography and 3D LGE images, employs a navigator gating technique to visualize small structures and pathologies, while avoiding the saturation effect and consequent SNR reduction.<sup>6,12–15</sup> In 3D phase contrast imaging, a navigator gating or respiratory gating technique is used to minimize the respiratory artifacts.<sup>16</sup> The navigator gating technique is also applied to 2–4 breath-hold 3D LGE or 3D tagging to maintain an identical diaphragmatic position between the breath-holds.<sup>17</sup>

<sup>1</sup>Department of Radiology, Nihon University Hospital, 1-6 Kanda-Surugadai, Chiyoda, Tokyo 101-8309, Japan

<sup>2</sup>Department of Radiology, Nippon Medical School, Tokyo, Japan

<sup>3</sup>Department of Cardiology, Nippon Medical School, Tokyo, Japan

<sup>4</sup>Department of Cardiology, Nihon University Hospital, Tokyo, Japan

<sup>5</sup>Department of Cardiology, Toho University Omori Medical Center, Tokyo, Japan

<sup>6</sup>Toshima Medical Center, Tokyo, Japan

\*Corresponding author, Phone: +81-3-3293-1711, E-mail: yas-amano@nifty.com

©2017 Japanese Society for Magnetic Resonance in Medicine

This work is licensed under a Creative Commons Attribution-NonCommercial-NoDerivatives International License.

Received: October 14, 2016 | Accepted: December 7, 2016

### **Parallel imaging or sparsity techniques**

Parallel imaging is usually used to reduce the examination time without compromising spatial resolution and cardiac phases.<sup>18–20</sup> Because a multichannel receiver coil is always used in cardiac MR imaging, parallel imaging, including sensitivity encoding (SENSE) and simultaneous acquisition of spatial harmonics, can be applied to 3D cardiac MR imaging. Once a reference scan with spatial and signal intensity information of the images is performed, the parallel imaging technique can be applied to any imaging sequence.<sup>19</sup> Although the SNR is reduced proportionally to the reduction factor used in the parallel imaging technique, the use of SSFP or gadolinium-based contrast agents can compensate for the reduction. In cine MR imaging, the k-t broad-use linear-acquisition speed-up technique (BLAST) or similar techniques are used to reduce the examination time by systematically omitting k-space data and by replacing the omitted data with that based on the assumption that the data may have similar signal intensity at various cardiac phases.<sup>9,19–22</sup> Another sparsity technique, such as compressed sensing, can omit further data not only in cine MR imaging but also in any other imaging sequence.<sup>23</sup> The reduction by parallel imaging is restricted by the channel numbers of the receiver coil, whereas the reduction by the k-t technique or that of sparsity data acquisition is not restricted. In 3D cardiac cine or LGE MR imaging, parallel imaging or sparsity techniques are necessary if the scan is to be kept tolerable for patients with heart failure.

### **SSFP**

SSFP is used in cine MR imaging and coronary MR angiography because of its high SNR, high blood signals, and shorter scan time.<sup>3,4,13,24</sup> Nonetheless, the SNR tends to be reduced in 3D SSFP MR imaging, especially when images are acquired during a single breath-hold, because the saturation effects are induced by a large number of phase encoding steps, short TR, and large flip angle.<sup>10</sup> Repeated breath-holding techniques with navigator gating may be a compromise for balancing acceptable SNR and scan time in coronary MR angiography.<sup>25</sup>

### **Gadolinium enhancement**

The administration of gadolinium-based contrast agents improves the SNR of MR images and contributes to the identification of many myocardial diseases. LGE MR imaging is the most valuable sequence for cardiac MR imaging, because it identifies myocardial scarring associated with various myocardial diseases.<sup>26,27</sup> Because of its shorter scan time, 3D LGE can be used as an alternative to multiple breath-holding 2D LGE.<sup>11</sup> The disadvantages of 3D LGE are sensitivity to motion artifacts because of its longer duration, possible insensitivity to subtle enhancement because of saturation effects, and lower spatial resolution.<sup>11,28</sup> Navigator-gated 3D LGE can provide the LGE images with high spatial resolution, and the combined use of phase sensitive inversion recovery (PSIR) may compensate for reduced contrast between the normal and scarred myocardium.<sup>14,15</sup> Gadolinium increases the SNR of

not only  $T_1$ -weighted gradient-echo imaging but also SSFP imaging because of reduced longitudinal relaxation time.<sup>5,29,30</sup> Therefore, gadolinium-based contrast agents can be used in the 3D cine cardiac MR imaging.

### **Presaturation**

Presaturation techniques, such as fat suppression and  $T_2$  preparation, are applied to 3D cardiac MR imaging to improve the SNR and contrast of acquired images. Presaturation techniques are always used in 3D coronary MR angiography to increase the contrast between epicardial coronary arteries and adipose tissue or myocardium adjacent to the arteries.<sup>6,7</sup> The presaturation pulses may be effective for suppressing respiratory and cardiac motion artifacts by nullifying signals from the chest wall, epicardial fat, and myocardium.

### **Spatial excitation**

Spatial excitation allows for images with a limited, smaller field-of-view (FOV) while avoiding phase wrapping artifacts.<sup>17,20,31</sup> In particular, spatial excitation is used for the second tagging preparation in 3D tagging, which allows for a half FOV without a wrapping-around artifact.<sup>17,32</sup>

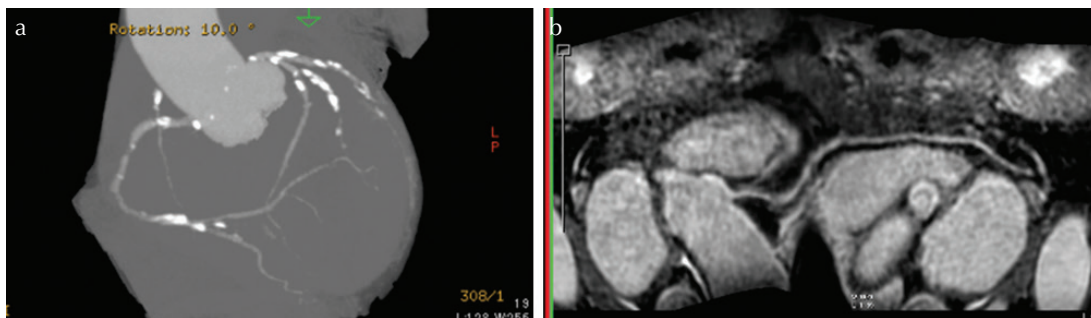
## **Clinical Application of Cardiac 3D Imaging**

### **Coronary MR angiography**

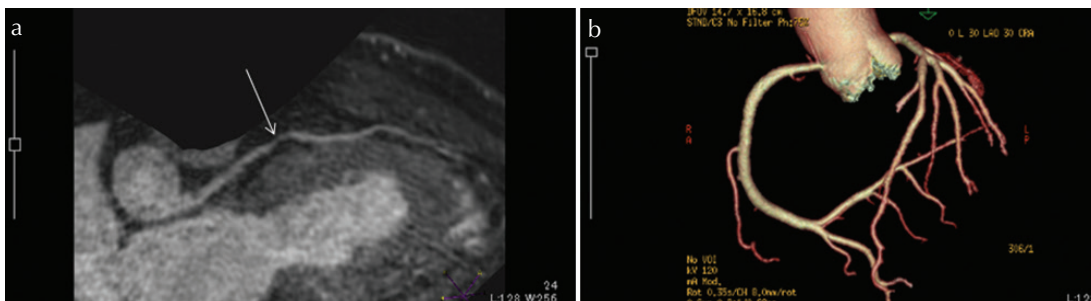
Coronary MR angiography is performed using ECG and navigator-gated 3D SSFP, and fat suppression and  $T_2$  preparation techniques.<sup>6,7</sup> These MR imaging techniques allow for higher spatial resolution, high blood signals with suppression of fat and myocardial signals adjacent to the arteries, and less image blurring. The advantages of 3D coronary MR angiography are its avoidance of contrast agents and irradiation, and its insensitivity to calcified plaques (Fig. 1). Although coronary MR angiography cannot estimate the calcium burden of the coronary arteries, it is able to evaluate the coronary artery stenoses adjacent to the calcified plaques. Compared with coronary CT angiography, the spatial resolution of 3D coronary MR angiography is coarse, its examination time is lengthy, the distance between the receiver coil and arteries can affect the vascular signals, and plaques cannot be readily identified.<sup>33</sup> Coronary artery stenosis may be estimated inaccurately using coronary MR angiography (Fig. 2).

### **Late gadolinium enhancement**

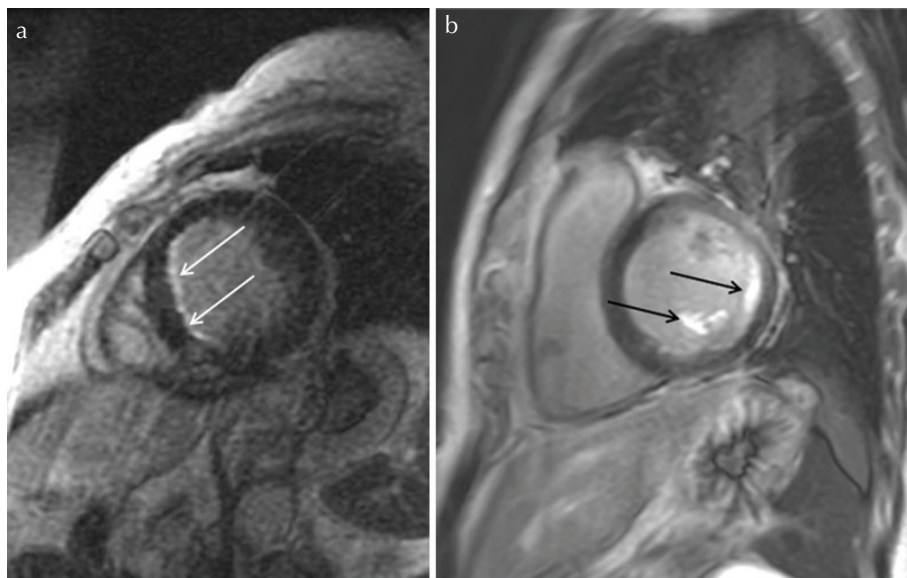
LGE is the most valuable tool among those for cardiac MR imaging, because it identifies myocardial scarring and inflammation.<sup>26,27,34</sup> LGE may be useful for differentiating cardiomyopathies with similar symptoms and predicting the prognosis of both myocardial infarction and nonischemic cardiomyopathies (Fig. 3a).<sup>26,27</sup> Multiple breath-holding 2D LGE is the standard imaging sequence, while single breath-holding 3D LGE can be used as an alternative with a shorter scan time (Fig. 3b). There are a few disadvantages associated with 3D LGE, such as sensitivity to



**Fig 1.** Coronary Computed Tomography (CT) angiography shows multiple calcified plaques of the coronary arteries, which obscure the accurate assessment of arterial stenosis (a). Three-dimensional (3D) coronary magnetic resonance (MR) angiography using steady-state free precession (SSFP) excludes stenoses of the coronary arteries (b).



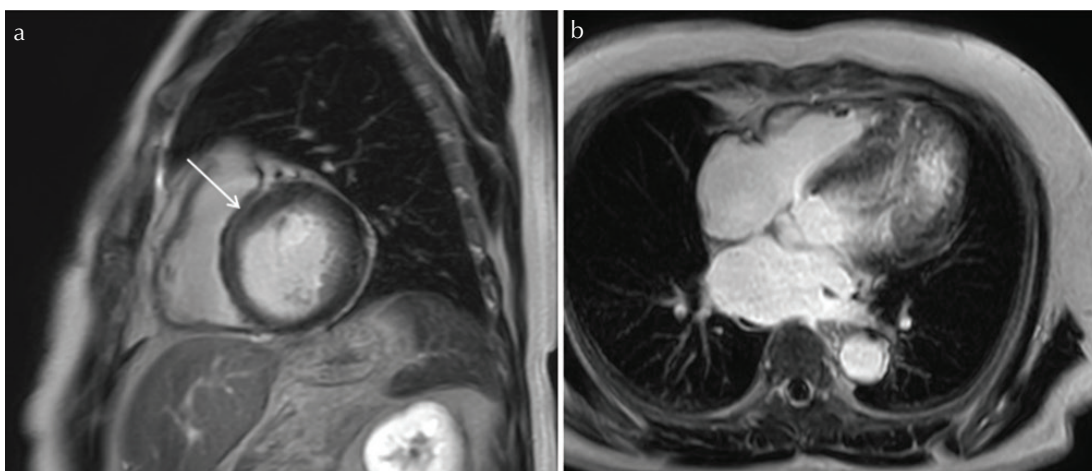
**Fig 2.** Mild coronary artery stenosis is suspected with three-dimensional (3D) coronary magnetic resonance (MR) angiography (a, arrow). However, coronary Computed Tomography (CT) angiography with high spatial resolution does not identify any coronary arterial stenosis (b). The voxel size of coronary MR angiography is  $0.46 \times 0.76 \times 1.6 \text{ mm}^3$ , while that of coronary CT angiography is  $0.41 \times 0.41 \times 0.63 \text{ mm}^3$ .



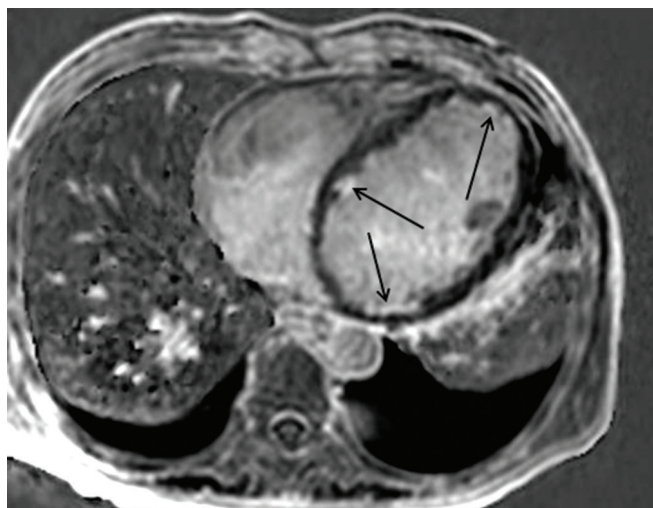
**Fig 3.** Short-axis two-dimensional (2D) late gadolinium enhancement (LGE) images show subendocardial myocardial infarction, which should be treated with an interventional procedure to recover the regional dysfunction (a, arrows). The imaging parameters of the 2D LGE are as follows: repetition time (TR), 6.1 ms; echo time (TE), 3.0 ms; flip angle,  $25^\circ$ ; in-plane resolution,  $1.59 \times 2.05 \text{ mm}^2$ ; and slice thickness, 5.0 mm. The 2D LGE requires 17 breath-holds to include the entire left ventricle. Short-axis three-dimensional (3D) LGE images, which require only 1–3 breath-holds, also show subendocardial and papillary muscular infarction (b, arrows). The imaging parameters of the breath-hold 3D LGE are as follows: TR, 3.9 ms; TE, 1.1 ms; flip angle,  $15^\circ$ ; in-plane resolution,  $1.40 \times 3.17 \text{ mm}^2$ ; and slice thickness, 10.0 mm.

image blurring from the longer duration time, possible insensitivity to subtle enhancement from saturation effects, and partial volume effect associated with lower spatial resolution (Fig. 4). The 3D LGE with 2–4 breath-holds may be a compromise between 2D LGE and single-breath-holding 3D LGE, which allows for higher spatial resolution and less saturation. Navigator-gated 3D LGE is another 3D LGE

imaging technique with high spatial resolution (Fig. 5), which can be used in patients with difficulty in holding their breath and allows for the MPR and simultaneous visualization of the myocardium and coronary arteries.<sup>14,15,35</sup> Navigator-gated 3D LGE is also used to visualize left atrial and pulmonary venous scarring after RF ablation for atrial fibrillation because of its high spatial resolution.<sup>36</sup> Because



**Fig 4.** Short-axis three-dimensional (3D) late gadolinium enhancement (LGE) images indicate myocardial scarring at the midwall of the basal anterior septal myocardium (**a**, arrows). However, a 4-chamber view LGE does not show any scarring (**b**), which indicates that the LGE represents a blurring artifact or septal perforator artery.



**Fig 5.** Navigator-gated three-dimensional (3D) late gadolinium enhancement (LGE) with phase sensitive inversion recovery (PSIR) reconstruction identifies multiple subendocardial myocardial infarction (arrows) and reflects the multiple vessel diseases. The imaging parameters of the navigator-gated 3D LGE are as follows: repetition time, 3.4 ms; echo time, 1.8 ms; flip angle, 15°; in-plane resolution, 1.5 × 1.25 mm<sup>2</sup>; and slice thickness, 2.5 mm. We use a 3.0T imager to maintain the image quality for small voxel size in the 3D imaging.

the scan time for navigator-gated 3D LGE is longer and gadolinium concentration in the blood changes during the data acquisition, PSIR can maintain the contrast between the normal and scarred myocardium (Fig. 5).<sup>15</sup>

### Cine SSFP

Multiple breath-holding 2D SSFP is a standard cine MR imaging sequence for estimating cardiac function and morphology (Fig. 6a). Single breath-holding 3D SSFP has been reported as an alternative cine imaging technique because of its shorter scan time.<sup>8–10</sup> The 3D cine SSFP with thin slice

thickness (e.g., <3 mm) is also available for MPR, while it always requires fast data acquisition, including SENSE with a high reduction factor, k-t BLAST, and compressed sensing, to reduce the breath-holding time.<sup>8–10,22</sup> Because of the repeated RF exposure associated with shorter TR and large flip angle used in 3D cine SSFP, the contrast between the blood and myocardium tends to decrease compared with 2D cine SSFP (Fig. 6).<sup>10</sup> The use of gadolinium can improve the image contrast on SSFP.<sup>29,30</sup> Image blurring is also observed in 3D cine imaging with a high reduction factor (Fig. 6c).

### Cine phase contrast

Cine phase contrast (PC) MR imaging is used to quantify the blood flow across the cardiac valves or intra- or extracardiac shunts, to visualize the flow direction in aortic dissection, and to estimate myocardial wall motion.<sup>16</sup> 3D cine PC or so-called four-dimensional (4D) Flow has several important advantages over 2D cine PC, including the avoidance of complicated slice orientation, volume data acquisition, and availability for various types of postprocessing (Fig. 7).<sup>16,37</sup> Because of the combined use of ECG and respiratory or navigator gating, the scan time of 3D cine PC is quite lengthy, usually over 10 min. The application of fast data acquisition techniques is unavoidable for reducing scan time appropriate for “clinical” 3D cine PC.<sup>37,38</sup>

### Tagging

Tagging MR imaging is valuable for evaluating the myocardial wall motion and strain quantitatively.<sup>39</sup> When using 2D tagging, multiple breath-holding should be performed to measure myocardial strain in several imaging slices and in 3 spatial dimensions. 3D tagging can be acquired only during 3 breath-holds (Fig. 8a). In 3D tagging, the navigator gating technique is used to maintain an identical diaphragmatic position during the breath-holds.<sup>12,17</sup> Echo-planar readout and the second tagging preparation using a spatial localized pulse are

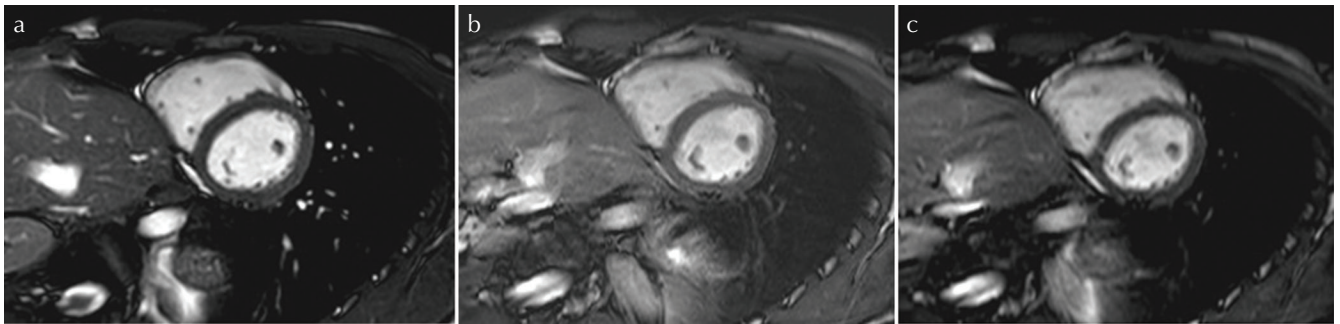


**Fig 6.** Multiple breath-hold two-dimensional (2D) cine steady-state free precession (SSFP) with a reduction factor of 2 (a) and single breath-hold three-dimensional (3D) cine imaging with a reduction factor of 4 in the phase direction (b), and that with a reduction factor of 5 (2.5 in the phase direction  $\times$  2 in the slice direction) (c). The 3D cine imaging requires a 16–20 sec breath-hold for 12 imaging slices. The contrast between the blood and myocardium is slightly lower in single breath-hold 3D cine imaging (b, c), compared with the standard 2D cine imaging (a). Image blurring is identified in 3D cine imaging with a higher reduction factor (c). The imaging parameters of the 2D cine SSFP are as follows: repetition time (TR), 2.8 ms; echo time (TE), 1.4 ms; flip angle, 50°; in-plane resolution, 1.98  $\times$  2.26 mm<sup>2</sup>; and slice thickness, 8.0 mm. The imaging parameters of the 3D cine imaging are as follows: TR, 3.5 ms; TE, 1.7 ms; flip angle, 50°; in-plane resolution, 1.70  $\times$  3.02 mm<sup>2</sup>; and slice thickness, 8.0 mm.

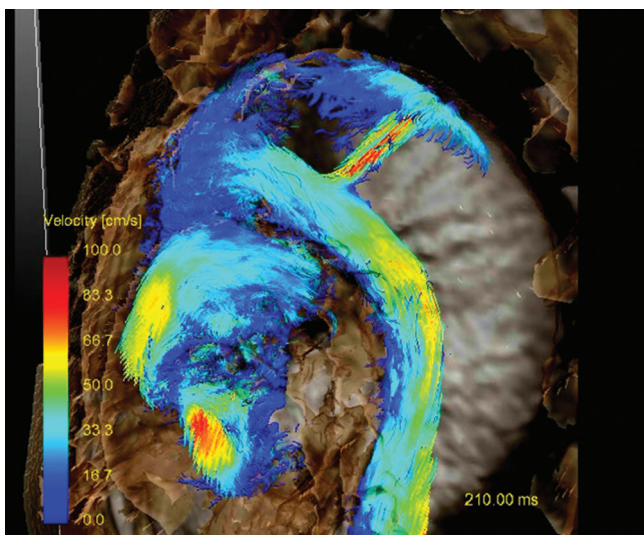


**Fig 7.** Electrocardiogram (ECG)-gated three-dimensional (3D) phase contrast magnetic resonance (MR) imaging showing turbulence close to the left ventricular outflow and jet flow across the intimal tear in a patient with aortic dissection. Because both ECG and respiratory gating techniques are used for 3D phase contrast imaging, the scan time is approximately 14 min.

applied to reduce the scan time significantly.<sup>31,32</sup> The 3D tagging can provide the 3D presentation of the entire left ventricle with grid tags (Fig. 8b), and has shown that the circumferential strain at the mid septal and posterior segments and apical segments in hypertensive cardiomyopathy is predominantly decreased, irrespective of the presence or absence of LGE.<sup>17</sup>

### Other cardiac MR imaging

Perfusion and T<sub>1</sub> and T<sub>2</sub> mapping are usually performed with 2D MR imaging sequences.<sup>40–42</sup> Therefore, both imaging methods are achieved at a single slice or 3–5 slices during a single breath-hold. The regional heterogeneity of myocardial perfusion, fibrosis or edema and small perfusion

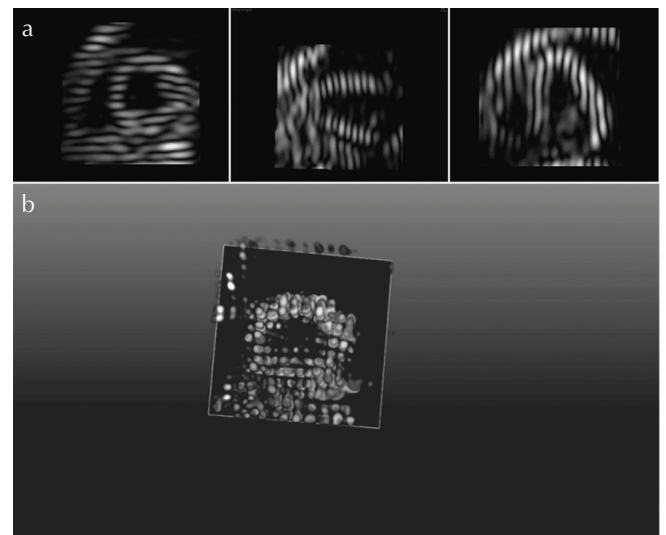


**Fig 8.** Echo-planar readout and the second tagging preparation using a spatially localized pulse are applied to three-dimensional (3D) tagging sequence. The cine images in 3 spatial directions are acquired during 3 breath-holds with navigator gating (a). The entire cardiac images with the grid tags are generated from the images with the line tags in the 3 directions. The cine 3D images with the grid tags show wall motion in a view from any angle and provide strain data for the region and the entire myocardium (b). A 3.0T magnetic resonance (MR) imager is used for the 3D tagging because the tags are maintained even at end-systole.

defects could be missed because of the limited slice coverage. Manka et al.<sup>43</sup> have reported that 3D perfusion imaging using k-t BLAST is able to include the entire heart and consequently visualizes the myocardial perfusion without an interslice gap. 3D T<sub>1</sub> mapping has been acquired using ECG and respiratory gating techniques, and therefore it requires approximately 5–8 min despite the use of parallel imaging.<sup>44</sup> Recently, 3D MR imaging using T<sub>2</sub> preparation and interleaved data acquisition (i.e., 3D-QALAS)

has been developed and is able to provide both  $T_1$  and  $T_2$  mapping of the entire myocardium within a single breath-hold.<sup>45</sup> Although these 3D MR imaging techniques should be validated in clinical situations, and postprocessing analyses should be developed to analyze the large amount of quantitative data effectively, they will allow for detailed evaluation of perfusion, fibrosis, and edema of the regional and entire myocardium associated with various myocardial diseases. 3D black-blood plaque imaging is still difficult to perform because of tortuosity of the coronary arteries and the data acquisition time. Recently, 3D non-contrast-enhanced heavily  $T_1$ -weighted imaging has been reported to visualize a vulnerable plaque of the coronary artery.<sup>46</sup> This imaging is acquired with 3D coronary MR angiography sequence modified by an inversion-recovery technique. Noguchi et al.<sup>46</sup> have reported that the 3D heavily  $T_1$ -weighted imaging can visualize the hyperintense coronary plaque that is related to the future cardiac events.

## Conclusions

3D cardiac MR imaging can be acquired by combining several MR imaging techniques, including ECG gating, fast data acquisition, and imaging sequences with high SNR. The 3D cardiac MR imaging may allow detailed evaluation of coronary arteries and small myocardial scarring or identification of the regional or global myocardial abnormalities without interslice gap and misregistration.

## Acknowledgments

This study was supported in part by the Grants-in-Aid for Scientific Research KAKENHI from the Japan Society for the Promotion of Science: Kiban (C) 26461838. The authors appreciate the technical support of Yoshio Matsumura, RT (Nippon Medical School Main Hospital) and Takeshi Yamamoto, RT (Nihon University Hospital). The authors also thank Gerard Crelier, PhD (GyroTools, Zurich, Switzerland) and Makoto Obara, RT (Philips Electronics Japan) for their advice and support regarding 3D tagging and cine phase contrast imaging sequences.

## Conflicts of Interest

All authors declared no conflict of interests related to this article.

## References

1. Davis CP, Hany TF, Wildermuth S, Schmidt M, Debatin JF. Postprocessing techniques for gadolinium-enhanced three-dimensional MR angiography. *Radiographics* 1997; 17:1061–1077.
2. Heiss SG, Shifrin RY, Sommer FG. Contrast-enhanced three-dimensional fast spoiled gradient-echo renal MR imaging: evaluation of vascular and nonvascular disease. *Radiographics* 2000; 20:1341–1352.
3. Carr JC, Simonetti O, Bundy J, Li D, Pereles S, Finn JP. Cine MR angiography of the heart with segmented true fast imaging with steady-state precession. *Radiology* 2001; 219:828–834.
4. Chavhan GB, Babyn PS, Jankharia BG, Cheng HLM, Shroff MM. Steady-state MR imaging sequences: physics, classification, and clinical applications. *Radiographics* 2008; 28:1147–1160.
5. Alley MT, Napel S, Amano Y, et al. Fast 3D cardiac cine MR imaging. *J Magn Reson Imaging* 1999; 9:751–755.
6. Brittain JH, Hu BS, Wright GA, Meyer CH, Macovski A, Nishimura DG. Coronary angiography with magnetization-prepared  $T_2$  contrast. *Magn Reson Med* 1995; 33: 689–696.
7. Simonetti OP, Kim RJ, Fieno DS, et al. An improved MR imaging technique for the visualization of myocardial infarction. *Radiology* 2001; 218:215–223.
8. Jung BA, Hennig J, Scheffler K. Single-breathhold 3D-true FISP cine cardiac imaging. *Magn Reson Med* 2002; 48:921–925.
9. Kozerke S, Tsao J, Razavi R, Boesinger P. Accelerating cardiac cine 3D imaging using k-t BLAST. *Magn Reson Med* 2004; 52:19–26.
10. Amano Y, Suzuki Y, van Cauwenhove M. Evaluation of global cardiac functional parameters using single-breath-hold three-dimensional cine steady-state free precession MR imaging with two types of speed-up techniques: comparison with two-dimensional cine imaging. *Comput Med Imaging Graph* 2008; 32:61–66.
11. Foo TK, Stanley DW, Castillo E, et al. Myocardial viability: breath-hold 3D MR imaging of delayed hyperenhancement with variable sampling in time. *Radiology* 2004; 230: 845–851.
12. Wang Y, Riederer SJ, Ehman RL. Respiratory motion of the heart: kinematics and the implications for the spatial resolution in coronary imaging. *Magn Reson Med* 1995; 33:713–719.
13. Sakuma H, Ichikawa Y, Chino S, Hirano T, Makino K, Takeda K. Detection of coronary artery stenosis with whole-heart coronary magnetic resonance angiography. *J Am Coll Cardiol* 2006; 48:1946–1950.
14. Amano Y, Matsumura Y, Kumita S. Free-breathing high-spatial-resolution delayed contrast-enhanced three-dimensional viability MR imaging of the myocardium at 3.0T: a feasibility study. *J Magn Reson Imaging* 2008; 28:1361–1367.
15. Kino A, Zuehlsdorff S, Sheehan JJ, et al. Three-dimensional phase-sensitive inversion-recovery turbo FLASH sequence for the evaluation of left ventricular myocardial scar. *AJR Am J Roentgenol* 2009; 193:W381–W388.
16. Markl M, Kilner PJ, Ebbers T. Comprehensive 4D velocity mapping for the heart and great vessels by cardiovascular magnetic resonance. *J Cardiovasc Magn Reson* 2011; 13:7.
17. Amano Y, Yamada F, Hashimoto H, Obara M, Asai K, Kumita S. Fast 3-breath-hold 3-dimensional tagging cardiac magnetic resonance in patients with hypertrophic myocardial diseases: a feasibility study. *Biomed Res Int* 2016; 2016:3749489.

18. Sodickson DK, Manning WJ. Simultaneous acquisition of spatial harmonics (SMASH): ultra-fast imaging with radiofrequency coil arrays. *Magn Reson Med* 1997; 38:591–603.
19. Pruessmann KP, Weiger M, Scheidegger MB, Boesiger P. SENSE: sensitivity encoding for fast MRI. *Magn Reson Med* 1999; 42:952–962.
20. Madore B. Using UNFOLD to remove artifacts in parallel imaging and in partial-Fourier imaging. *Magn Reson Med* 2002; 48:493–501.
21. Tsao J, Boesinger P, Pruessmann KP. k-t BLAST and k-t SENSE: dynamic MRI with high frame rate exploiting spatiotemporal correlations. *Magn Reson Med* 2003; 50:1031–1042.
22. Okuda S, Yamada Y, Tanimoto A, et al. Three-dimensional cardiac cine imaging using the kat ARC acceleration: initial experience in clinical adult patients at 3T. *Magn Reson Imaging* 2015; 33:911–917.
23. Lustig M, Donoho D, Pauly JM. Sparse MRI: The application of compressed sensing for rapid MR imaging. *Magn Reson Med* 2007; 58:1182–1195.
24. Scheffler K, Lehnhardt S. Principles and application of balanced SSFP technique. *Eur Radiol* 2003; 13:2409–2418.
25. Matsutani H, Amanuma M, Sekina T, Kondo T, Kuhara S, Takase S. Coronary whole-heart MR angiography: feasibility of breath-hold chasing with diaphragmatic navigation. *Magn Reson Med Sci* 2016; 15:340–345.
26. Kim RJ, Wu E, Rafael A, et al. The use of contrast-enhanced magnetic resonance imaging to identify reversible myocardial dysfunction. *N Engl J Med* 2000; 343:1445–1453.
27. Mahrholdt H, Wagner A, Judd RM, Sechtem U, Kim RJ. Delayed enhancement cardiovascular magnetic resonance assessment of non-ischaemic cardiomyopathies. *Eur Heart J* 2005; 26:1461–1474.
28. Turkbey EB, Nacif MS, Noureldin RA, et al. Differentiation of myocardial scar from potential pitfalls and artefacts in delayed enhancement MRI. *Br J Radiol* 2012; 85:e1145–e1154.
29. Lasalarie JC, Serfaty JM, Carre C, et al. Accuracy of contrast-enhanced cine-MRI sequences in the assessment of left ventricular function: comparison with precontrast cine-MRI sequences. Results of a bicentric study. *Eur Radiol* 2007; 17:2838–2844.
30. Amano Y, Yamada F, Kitamura M, et al. Contrast-enhanced steady-state free precession in the assessment of hypertrophic obstructive cardiomyopathy after alcohol septal ablation. *Magn Reson Med Sci* 2016; 15:130–136.
31. Alley MT, Pauly JM, Sommer FG, Pelc NJ. Angiographic imaging with 2D RF pulses. *Magn Reson Med* 1997; 37:260–267.
32. Rutz AK, Ryf S, Plein S, Boesiger P, Kozerke S. Accelerated whole-heart 3D CSPAMM in myocardial motion quantification. *Magn Reson Med* 2008; 59:755–763.
33. Hamdan A, Asbach P, Wellnhofer E, Klein C, Gebker R, Kelle S, et al. A prospective study for comparison of MR and CT imaging for detection of coronary artery stenosis. *JACC Cardiovasc Imaging* 2011; 4:50–61.
34. Abdel-Aty H, Boye P, Zagrosek A, et al. Diagnostic performance of cardiovascular magnetic resonance in patients with suspected acute myocarditis. *J Am Coll Cardiol* 2005; 45:1815–1822.
35. Amano Y, Kiriya T, Kobayashi Y, Tachi M, Matsumura Y, Kumita S. Simultaneous assessment of myocardial scar and coronary arteries using navigator-gated 3-dimensional fat-suppressed delayed-enhancement MRI at 3.0 T: a technical feasibility study. *J Comput Assist Tomogr* 2012; 36:72–76.
36. Peters DC, Wylie JV, Hauser TH, et al. Recurrence of atrial fibrillation correlates with the extent of post-procedural late gadolinium enhancement: a pilot study. *JACC Cardiovasc Imaging* 2009; 2:308–316.
37. Hsiao A, Justig M, Alley MT, et al. Rapid pediatric cardiac assessment of flow and ventricular volume with compressed sensing parallel imaging volumetric cine phase-contrast MRI. *AJR Am J Roentgenol* 2012; 198:W250–W259.
38. Sekine T, Amano Y, Takagi R, Matsumura Y, Murai Y, Kumita S. Feasibility of 4D flow MR imaging of the brain with either Cartesian y-z radial sampling or k-t SENSE: comparison with 4D flow MR imaging using SENSE. *Magn Reson Med. Sci* 2014; 13:15–24.
39. Jeung MY, Germain P, Croisille P, El ghannudi S, Roy C, Gangi A. Myocardial tagging with MR imaging: overview of normal and pathologic findings. *Radiographics* 2012; 32:1381–1398.
40. Greenwood JP, Maredia N, Younger JF, et al. Cardiovascular magnetic resonance and single-photon emission computed tomography for diagnosis of coronary heart disease (CE-MARC): a prospective trial. *Lancet* 2012; 379:453–460.
41. Messroghli DR, Walters K, Plein S, et al. Myocardial T<sub>1</sub> mapping: application to patients with acute and chronic myocardial infarction. *Magn Reson Med* 2007; 58:34–40.
42. Wassmuth R, Prothmann M, Utz W, et al. Variability and homogeneity of cardiovascular magnetic resonance myocardial T<sub>2</sub>-mapping in volunteers compared to patients with edema. *J Cardiovasc Magn Reson* 2013; 15:27.
43. Manka R, Jahnke C, Kozerke S, et al. Dynamic 3-dimensional stress cardiac magnetic resonance perfusion imaging. *J Am Coll Cardiol* 2011; 57:437–444.
44. Coniglio A, Di Renzi P, Freixas V, et al. Multiple 3D inversion recovery imaging for volume T<sub>1</sub> mapping of the heart. *Magn Reson Med* 2013; 69:163–170.
45. Kvernby S, Warntjes MJB, Haraldsson H, Carlhäll CJ, Engvall J, Ebbens T. Simultaneous three-dimensional myocardial T<sub>1</sub> and T<sub>2</sub> mapping in one breath hold with 3D-QALAS. *J Cardiovasc Magn Reson* 2014; 16:102.
46. Noguchi T, Kawasaki T, Tanaka A, et al. High-intensity signals in coronary plaques on noncontrast T<sub>1</sub>-weighted magnetic resonance imaging as a novel determinant of coronary events. *J Am Coll Cardiol* 2014; 63:989–999.